9.11 SEA-SALT SIZE-DISTRIBUTIONS FROM BREAKING WAVES: IMPLICATIONS FOR MARINE AEROSOL PRODUCTION AND OPTICAL EXTINCTION MEASUREMENTS DURING SEAS

Antony Clarke*, V. Kapustin, S. Howell, K. Moore, B. Lienert[1], S. Masonis[2], T. Anderson[2], D. Covert[2], K. Shifrin[3], I. Zolotov[3]

Department of Oceanography, University of Hawaii, Honolulu, HI
[1]Hawaii Institute of Geophysics and Planetology, University of Hawaii, Honolulu, HI
[2]Department of Atmospheric Sciences, University of Washington, Seattle, WA
[3]College of Oceanic & Atmospheric Sciences, Oregon State University, Corvallis OR

1. INTRODUCTION

The Shoreline Environmental Aerosol Study (SEAS) place at Bellows Air Force Station (BAFS) on the east coast of Oahu, Hawaii between April 16 and May 1, 2000. The site description, sampling considerations, environmental factors influencing coastal aerosol production and SEAS participants are discussed elsewhere (Clarke and Kapustin, 2002). Here we focus on marine aerosol size distributions and their link to optical properties. A variety of instruments were used over the size range from 10nm to over 10μm that span 10 orders of magnitude in aerosol mass. We will first address the smallest size range below about 0.1μm that was found to dominate sea-salt number and then the larger range 0.1 to several μm that frequently contribute to near-surface marine aerosol mass and its optical properties.

The University of Hawaii (UH) sampling was carried out from the 20m BAFS tower (Figure 1a) through an 8cm diameter PVC sample line that carried aerosol to our research van that housed our instruments at the base of the tower. Three solenoid diaphragm valves with large cross section of about 4 cm^2 were mounted on the tower to provide selective sampling form 5, 10 and 20m (7, 12, and 22m asl) elevations. Valve was sampled sequentially for 20 minutes out of each hour in order to obtain both temporal and vertical variations in the aerosol field. The bottom valve was generally influenced by nearby shoreline breaking waves (Fig. 1b) while the higher valves were not, even though all were often influenced by other sources such as the upwind reef.

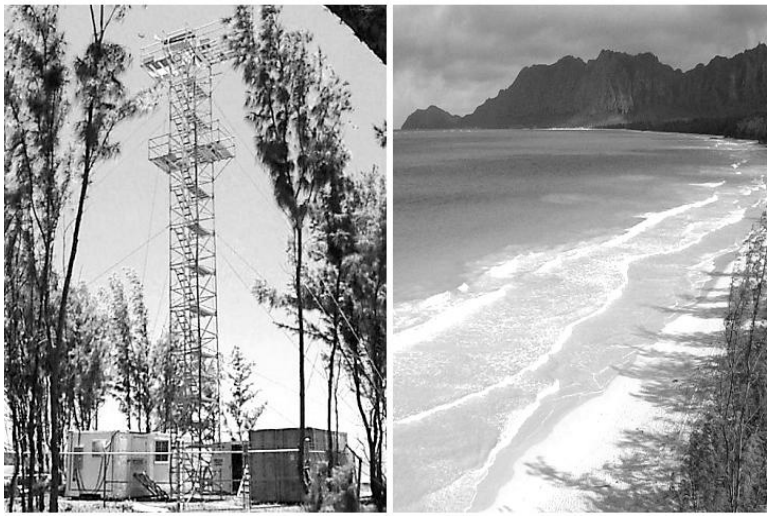

Figure 1. View from the landward side of the BAFS 20m sampling tower with UH inlets at 5, 10 and 20m and view of the coastal breaking waves taken from top of the tower.

The UH sample line terminated inside the portable laboratory van at the base of the tower. Several smaller tubes were mounted near the center of the PVC sample line flow with diameters selected to allow for near isokinetic sampling to various instruments. The largest flow of 30 lpm went to a three-wavelength integrating nephelometer (Mod. 3551 TSI Inc.) that alternately inserted an impactor with aerodynamic size cut at 1 μm. This generally operated near 55% relative humidity compared to ambient values that were usually in the 70-85% range. Another enclosed

* Corresponding author address: Antony Clarke, Department of Oceanography, University of Hawaii, 1000 Pope Rd. Honolulu, HI 96822;
e-mail: tclarke@soest.hawaii.edu

nephelometer [University of Washington, UW] near 10m on the tower operated near ambient RH (Masonis et al., 2002). Two condensation nuclei, CN, counters recorded particle number concentrations at 40°C (CNcold) and 360°C (CNhot). Refractory particles remaining after heating to 360°C, such as sea salt, could be distinguished from more volatile species such as sulfates at up to 1Hz time resolution. Other supportive measurements such as wind speed, wind direction, relative humidity, precipitation, tides, pressure, sunlight and meteorological parameters were also recorded.

Size distributions were determined with an aerosol particle spectrometer (APS Mod. 3320, TSI Inc.; 0.5<Dp<10μm), radial differential mobility analyzer (RDMA; 0.007<Dp<0.3μm) and a laser optical particle counter (OPC; 0.1<Dp<7μm). Both of the latter employed thermal volatility to measure distributions in air sampled at 40, 150 and 300°C. This established the volatile particle fractions (Clarke, 1991) and isolated the sea-salt distribution refractory at 360°C. The RDMA was used in conjunction with a LAG (Lagged Aerosol Grab) chamber that "captured" a sample of air over about 15s for subsequent analysis over several minutes at three temperatures. This ensured that small-scale temporal variation in the sample did not occur during the 3 min measurement period, a critical requirement to sample wave breaking plumes of 15-60s duration.

The UH lidar operated over a range of angles, distances and altitudes during SEAS and detected aerosol produced from breaking waves (if focused just downwind of the reef or along the coast) to open ocean conditions (Porter et al., 2000, Porter et al., 2002). Because a major SEAS objective was to link in-situ data to lidar observations, many lidar measurements were carried at about a 58deg. azimuth in a vertical scanning mode to explore vertical development of aerosol plumes downwind of the reef and moving toward the tower. Even so, the variable wind directions, speeds and aerosol plume structures (Clarke and Kapustin, 2002, Porter et al., 2002) meant that the lidar and the wind direction bringing aerosol to the tower were in alignment only rarely. Also, since plumes evolve, mix and dilute during transport from where the lidar intercepted them to the tower a direct comparison of these measurements are problematic. Here we describe a long-term statistical assessment by sampling from the three tower locations as a means to evaluate in-situ and lidar extinction data. This provided data ranging from conditions similar to breaking waves collected near the bottom of the tower to approximately open-ocean conditions by sampling at the top (20m). Of course, when waves were breaking on the offshore reef about 1.6 km away even the 20m data could be influenced by aged plumes from the reef.

Hence, the UH measurements could observe production of near-shore aerosol produced from isolated breaking waves at the base of the tower after removing the open ocean contribution derived from the top of the tower. This allowed direct assessment of the impact of shoreline breaking waves on aerosol production as a function of size. These waves were generally small during the SEAS period (ca. 0.5m) and break about 20-25m from the shore to produce foam for about 20-30s before dissipating on the shore (Fig. 1b). These wave heights were often less than wave heights in the reef region but the 20m foam exposure is also similar to that on the reef about 1.5km away allowing us to use breaking wave data from the lowest tower inlet as a surrogate for contributions from similar waves from the reef region.

2. SAMPLING ISSUES

Quantitative comparisons of independently measured and remotely sensed properties require proper calibrations, corrections and transformations to appropriate measurement conditions. The change in marine aerosol size with relative humidity (RH) is one issue that affects many physical, chemical and optical properties examined in SEAS. Water uptake influences aerosol size, density and refractive index in ways that impact the interpretation of data from various instruments and its extrapolation to ambient conditions. Some sizing instruments are nominally "dry" in the sense that they measured at low (but often different) RH with relatively little water volume associated with them. Other instruments (eg. nephelometers) were at intermediate humidity while lidar and visibility were at ambient conditions near 80%RH.

The DMA, OPC and APS size distributions were measured at instrument RH. The DMA employed dessicated sheath air sample flow to bring RH to about 25% for sizing. The OPC mixed sample and dessicated air upstream of the instrument to lower RH to about 40%. The APS internal heating to 30-32°C resulted in RH near 50% but generally above the efflorescence point of sea-salt (Tang et al, 1997). Obtaining size distributions from these instruments for modeling optical properties and/or comparison purposes require a number of steps. Original calibration for all instruments employed latex calibration spheres with a refractive index of 1.588 and density of 1.05 g cm^{-3}. After adjustments to "dry" (RH=40%) diameters we combined these instruments to provide sizing over the ranges 0.007 to 0.15, 0.15-0.75 and 0.75-12.0 μm respectively. These generally include one or more corrections for a) measured vs. calibration aerosol properties, b) measured vs. desired humidity conditions, c) size dependent instrument performance and d) size dependent sampling (Clarke et al., 2002)

3. OBSERVATIONS

3.1 Representative Tower Data and Aerosol Microphysics

Measurements from the various tower altitudes revealed clear differences in number concentrations, particle volumes and associated optical properties (Figure 2). At the lowest altitude (valve t1), excursions

in CN of about 50 cm^{-3} are associated with production from breaking waves.

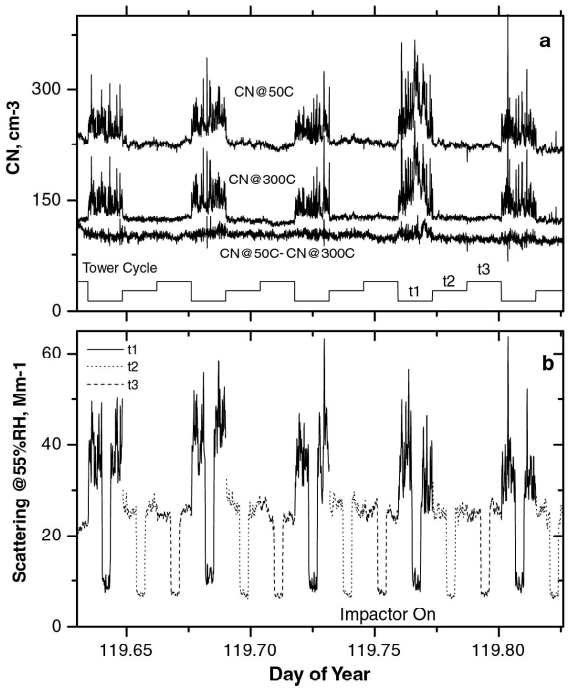

Figure 2a shows an example of cycling through the three tower valves over a 5 hour period for measured CNcold, CNhot and their difference.

Heated CN show similar excursions while the difference between heated and unheated CN are nearly constant and similar to values at heights unperturbed by these breaking waves. Hence, most CN are refractory as expected for a sea-salt aerosol at 360°C and superimposed upon a more stable and more volatile background aerosol. Aerosol light scattering (corrected for truncation errors) for the same period (Figure 2b) is interrupted by a 5min period when the impactor [1μm aerodynamic cut size] is inserted into the flow to reveal the submicrometer scattering data. These data also show that shoreline waves enhance scattering at 5m by up to a factor of two compared to other levels. The impactor data for the lowest valve, t1, shows an enhancement of 30 $\pm$ 10% compared to other levels and indicates the optical influence of submicrometer sea-salt aerosol at 550nm. The 10m and 20m tower data are similar but with occasional enhancements of 10% for the 10m inlet position, indicating weak but occasional breaking wave influence at this altitude.

An expanded one-hour time series sampled every 5s (Figure 3 a,b) better reveals concurrent variations in both CN and nephelometer light scattering (ca. 55%RH) at all three tower altitudes including 5 minute impactor data. However, the nephelometer internal volume (ca. 3l), the 30 lpm flow rate and the internal temporal averaging of 10s results in an effective delay of about 15s and a smoothing (broadening) of scattering compared to CN data. The 5s CN data at 5m better resolves aerosol plume structures as short as 15s or with overlapping peaks lasting up to about a minute, consistent with variable production from multiple waves breaking along the shore (Fig. 1b).

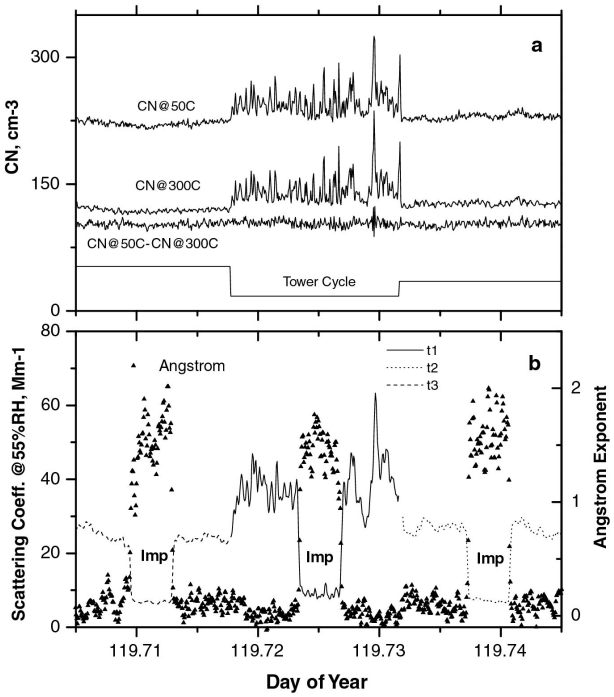

Figure 3. A one hour time series showing a) CNcold, CNhot and their difference and b) scattering extinction and Angstrom exponent data for each 20min valve cycle.

Concurrent excursions in CNhot and CNcold for breaking waves at 5m (Fig. 3a) show similar magnitudes for each wave breaking event. The difference between CNcold and CNhot (more volatile number fraction) is nearly constant and reflects a different origin for these more volatile nuclei at all tower altitudes. These features demonstrate that wave produced particles are all refractory, as expected for sea-salt at 360C. Excursions in these salt nuclei concentrations at 5m typically range from about 20 to over 100 cm^{-3} for these small coastal waves. Concurrent variations are evident in CN and light scattering data (slightly delayed and broadened) for both total and submicrometer aerosol at 5m. These waves break, produce foam and dissipate over about 20m (Fig. 1b) and enhance the 5m CN concentrations at the tower by about 25-50% and light scattering by about 50-100% over open ocean values. However, as shown below, the light scattering is dominated by a very small percentage of particle number present in the large particle size range.

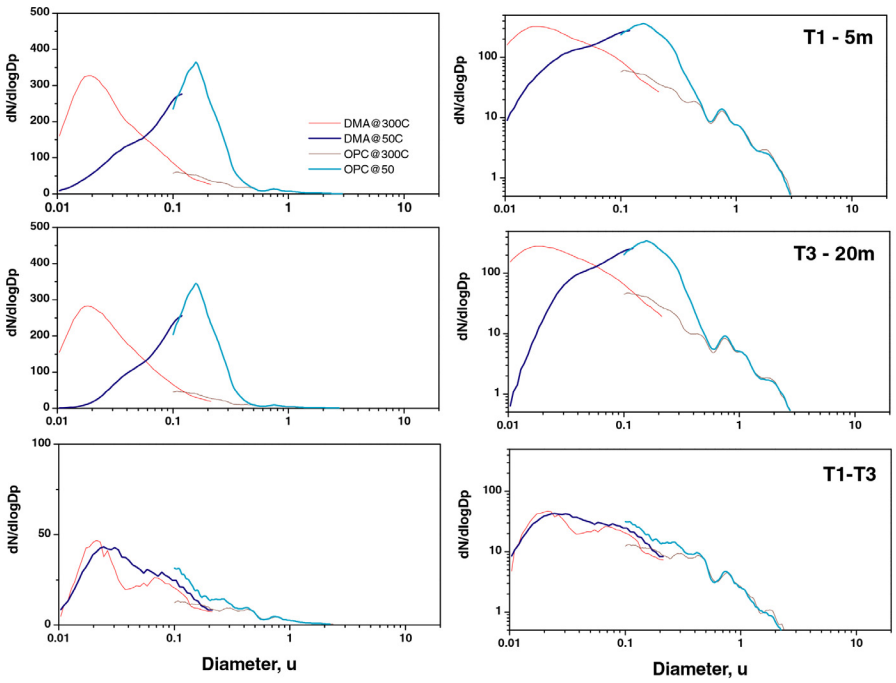

Figure 4a,b Dry number size distributions (DOY119) measured at 20m, 5m and their difference (lower panels) for unheated (40°C) and heated refractory distributions (360°C) in linear and logarithmic concentration formats (10 point diameter smoothing applied).

The wavelength dependence of light scattering measured by the UH TSI nephelometer can be described by the Angstrom exponent [see Masonis et al. 2002] which tends to values near zero for large aerosol and to values near 2 when only small aerosol are dominant. The Angstrom exponent for this 1 hr period is shown in Fig. 3b where the impactor demonstrates this variation when large aerosol are removed. The large contributions of coarse aerosol to the total scattering at all altitudes (Fig 2b) is also revealed here with Angstrom exponents near zero for all tower altitudes. Lowest values are most evident for 5m altitude data and short period increases in scatter from breaking wave events can drive the Angstrom exponent to its lowest values (eg. see data near DOY 119.73). Smaller excursions in the CN cold, CN hot and scattering are also evident even at the 10m and 20m altitudes.

3.2 Size Distributions Produced from Breaking Waves

As described earlier, the full size-distributions from 7nm to over 10μm were obtained from a combination of instruments including the RDMA and OPC equipped with thermal analysis to help resolve refractory constituents and to infer composition (Clarke, 1991). In order to extract size distributions for aerosol produced only from the breaking waves at 5m described above we examined differences between average size distributions accumulated at the top of the tower and the bottom.

Here we show (Figure 4) results of such an assessment for the 5 hr period on DOY119 shown above (Fig. 2).

In the linear format of dN/dlogDp vs. logDp the area under the curves are proportional to total number and best reveal the small particle contribution while the logarithmic format provides size information over a greater range of particle sizes.

The heated distributions at both tower altitudes are shifted to much smaller sizes for particles below about 0.5 μm while larger sizes are relatively unaffected. These large sizes are refractory sea-salt while smaller sizes are generally mixtures of sea-salt with volatile species (eg. sulfates) and other components. Since DOY119 is during the period of long-range transport (Clarke and Kapustin, 2002) refractory species other than sea salt are likely.

The contribution of coastal breaking waves is clearly revealed by the difference between the 20m and 5m number distributions (Fig. 4 lower panels). The unheated difference distribution demonstrates that breaking waves produce particles from as small as 10nm (dry diameter) up to several micrometers (larger sizes not shown here) and with a number peak near 30nm. The heated difference distributions (lower panel) show these are all refractory at 300C, consistent with their being sea-salt. The fact that both heated and unheated averaged distributions are nearly identical demonstrates that virtually all particles produced are refractory sea-salt. The integral number of about 35 cm^{-3} is consistent with the typical number peaks in the CNcold and CNhot from breaking waves at the 5m level (Figure 3). The shape of these difference distributions are also similar to the refractory distributions observed at both altitudes and suggests that sea-salt in open-ocean conditions also contribute to these refractory aerosol.

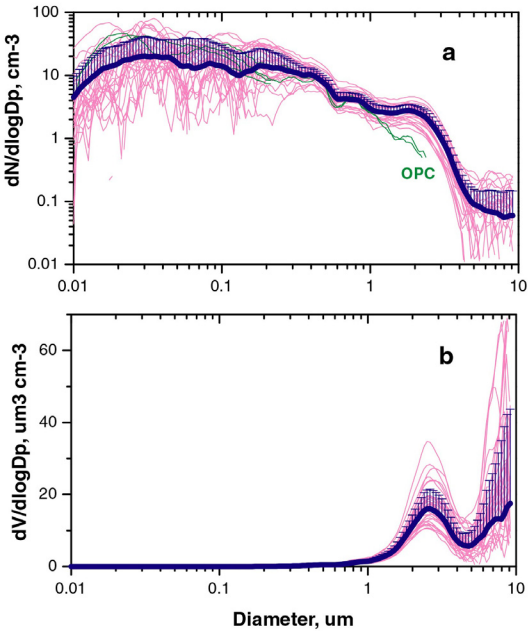

Figure 5. All "dry" number and volume size distributions obtained by differencing the average 5m and 20m tower data obtained from each hourly cycle during SEAS and after applying the transmission correction to the UH inlet discussed below.

Coarse particles from breaking waves were also characterized through differencing the data collected at the top and bottom of the tower. However, because concentrations are low for coarse aerosol we use averages for each 20min sample from each altitude over many hourly cycles. These coarse particle distributions also require some corrections for inlet losses. These are shown in Figure 5a as number distributions on a logarithmic scale but the sea salt mass and sizes most effective optically are best revealed in Figure 5b as linear volume distributions [Multiply scale by about 2 to estimate dry mass distributions in $\mu g\ m^{-3}$]. These difference distributions show that these coastal breaking waves produce aerosol dry mass peaked near 3μm with an additional "giant" mode suggested near 10μm also evident in other coastal data (de Leeuw et al., 2000). However, we believe that this mode is exaggerated in our measurements as a result of "ghost" particles often present in Model 3320 APS data (see below).

3.3 Comparison of in-situ data with lidar extinction

This "closure" provides a basis for modeling aerosol optics at ambient conditions, as needed for comparison to lidar data. The details of the lidar retrievals (Porter et al., 2002) are discussed elsewhere and will not be repeated here nor will the independent evaluations of the lidar backscatter coefficient (Masonis et al, 2002). Direct comparisons of in-situ tower data and lidar measurements during SEAS are complicated by the fact that the lidar data is obtained from some region 300-400m or more offshore. Even when favorable winds advect aerosol from a region (eg. the reef) to the tower, allowing a direct comparison of lidar extinction with the nephelometer extinction and size distributions, a quantitative comparison is questionable due to the roles of mixing, dispersion, dilution and meandering winds (see Clarke and Kapustin, 2002; Porter et al., 2002).

Since such optimal periods are uncommon and their interpretation uncertain we argue that effective comparisons can be based upon the variations in aerosol and scattering observed for various tower altitudes. We earlier described how breaking wave events (Fig.1) measured at 5m have similar time scales and surface foam exposure as those on the reef. Hence, the impact of the larger "reef" breaking waves on lidar extinction downwind of the reef is similar in character and duration to the 5m tower data and should gradually decrease during transport away from the reef. Also, the 20m tower data that often reflect open ocean conditions should correspond to minimum values in lidar extinction where impact from "reef" breaking waves is negligible. Hence, we argue here that most lidar extinction data collected during SEAS should exhibit values that fall between extinction determined from our 5m and 20m tower data and the long-term variation in the minimum values bounded by the 20m tower measurements should be consistent with similar long-term variations in the lidar data.

During each 2 min vertical lidar scan the data was averaged (5s) over a swath 25m high and 100m along the beam located about 300-400m out from tower at an angle of 58° (toward reef – Fig. 1b). At a nominal wind speed of 10 ms^{-1} about 100 linear meters of air will pass our sample inlet for each 10s sample interval in the tower data. This means a single measurement representing the lidar "swath" is generally comparable to two 5s in-situ data points at the tower. Even so, values between the surface and 25m are mixed in the lidar "swath" and parcels of this air may or may not move inland to tower. As mentioned earlier, during SEAS the airflow from the most active reef area tended to pass north of the tower. Aerosol plumes from the reef area could also lift quickly, mix and dilute during passage to tower (Porter et al., 2002). However, minimum values in lidar and tower extinction data should reflect values least influenced by recent breaking waves. At the same time, pronounced increases in lidar values caused by aerosol plumes from the reef regions should approach peak excursions in tower extinction data associated with the coastal waves as characterized at the 5m tower height. Horizontal lidar data for waves along the beach (Porter et al., 2002) tended to reach to only about 4m high near the waters edge but with perturbed flow over the research vans at the tower (Fig 1a) these plumes were clearly evident in our 5m data (Fig. 2, 3) but perhaps diluted compared to undisturbed plumes. Nevertheless, the range of

values at 5m is expected to bound lidar values at 300m and reveal similar overall trends. Given the good agreement established above between measured nephelometer extinction and the values calculated from the size distributions then both nephelometer and size-derived extinction, after correction to ambient conditions, should bracket the range of variations in lidar extinction.

Figure 6 shows UH nephelometer data corrected to obtain expected ambient scattering extinction after allowing for angular truncation (Anderson and Ogren, 1998), sampling losses and f(RH) for the SEAS period, as discussed earlier. Because the nephelometer did not measure some of the largest aerosol due to inlet losses discussed above, the measured scattering will be less than it should be. However, based upon size dependent losses characterized above we estimate about a 22% increase in scattering expected under ambient conditions and has been applied to the ambient nephelometer values shown. Continuous scattering data for 5m data reveal the high values and large variability associated with intermittent breaking waves in contrast to the lower and less variable data for the 20m sampling. Also shown are extinction values calculated from the size distributions taken from 5m and 20m corrected to ambient conditions. Most values for the ambient 20m calculated scatter (green squares) agree well with the ambient corrected nephelometer values. The size-derived extinction at 5m (20 min avg.) for breaking waves (triangles) also often show good agreement and generally centered on the excursions in the 5m nephelometer data. Lidar extinction (5s avg. taken every 2 minutes - open circles) from the 25m by 100m lidar swath are shown (Figure 6) when available. The lower envelope of many lidar values fall near the 20m extinction values obtained from the size distributions and nephelometer extinction data (e.g. DOY 13.7-13.9, 15.5-15, 15.8-16.4, 119.5) but frequently lidar values show excursions to somewhat higher values in these periods that are not seen in the 20m tower data.

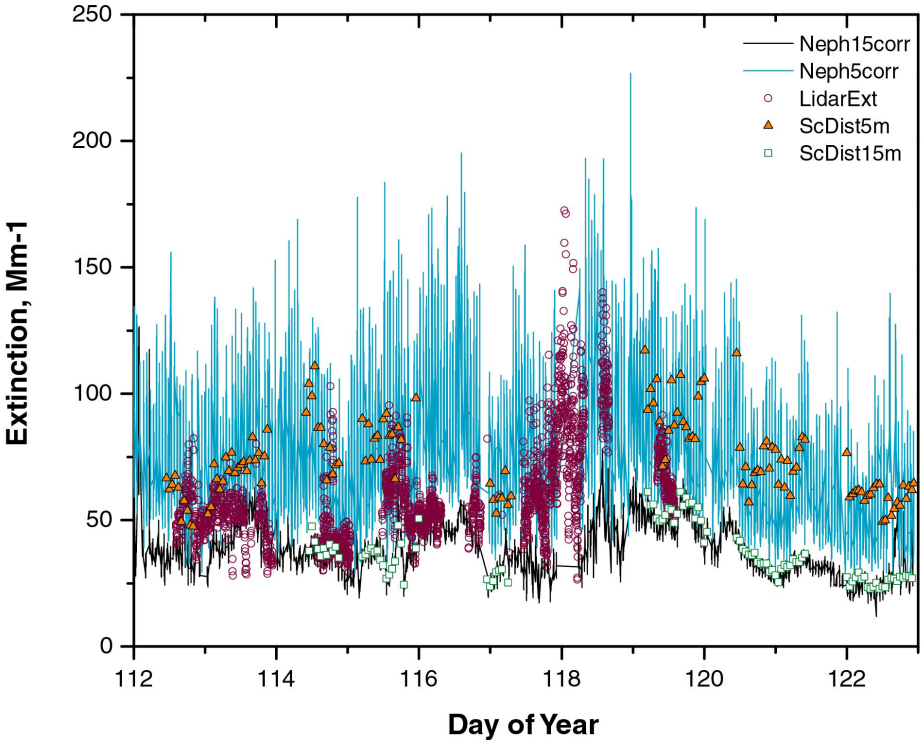

Figure 6. SEAS time series of 5m and 20m continuous extinction data corrected to ambient conditions (thin lines) with corresponding extinction calculated with 20min averages from size distribution (boxes) compared to variations in lidar extinction observed 300-400m offshore from 0-25m (circles).

The larger excursions in lidar data generally fall within the highly variable 1-2 min nephelometer extinction peaks at 5m (also see Fig.2) but close to the averaged (20min) size-distribution extinction at 5m. Sequential lidar values often range quickly over several minutes consistent with plume features meandering in and out of lidar box and being resampled every 2 minutes.

4. CONCLUSIONS

By sampling sequentially at three tower altitudes over an extended period we were able to characterize the size distributions derived from individual near surface breaking wave events from the background marine aerosol. Isolating these event by means of a LAG chamber and applying thermal analysis to identify their refractory properties we were able to demonstrate sea-salt from breaking waves were produced in all sizes between 10nm to greater than 10μm. These distributions were similar for

heated and unheated distributions confirming their refractory nature at 300°C as expected for sea-salt. The typical number concentrations for integrated size distributions from small breaking wave events were in the range of 30-50 cm^{-3} and consistent with spikes in concurrently collected total CN number concentrations. The shape of this breaking wave number distribution was also similar that of the refractory distribution characteristic of the open ocean data collected at the top of the tower. This suggests that open ocean breaking waves may contribute significantly to open ocean particle number and become incorporated into mixed refractory and volatile particles trough heterogeneous chemical reaction on the sea-salt surface and/or coagulation with a more volatile aerosol often entrained from above the marine boundary layer (Clarke et al., 1996). Due to the high diffusivity of the smaller sea-salt (say diameters below 0.05μm) produced by breaking waves it is more likely that they are removed to preexisting marine aerosol surface while the larger aerosol could more readily be involved in heterogeneous reactions and act as cloud condensation nuclei under typical marine conditions. Small coastal breaking waves also produced particles with sizes larger than 1μm that are more commonly observed. These contributions were at far lower concentrations and on the order of 1 cm^{-3} but interact effectively with visible light and generally enhanced the aerosol light scattering (550nm) by about a factor of two at 5m about 20m downwind of the waters edge. Hence, production of these larger sea-salt aerosol can dominate scattering extinction in a coastal setting over moderate spatial scales when breaking waves are present (Clarke et al., 2003).

Offshore variability in response to breaking waves was also evident in lidar data near the reef. Long term comparisons were made between of the range of extinction values obtained by lidar between the reef and tower and the range of extinction measured at the tower for both near-shore breaking waves at 5m and unperturbed values made at 20m. Lidar extinction values averaged over a 50m square swath about 300-400m offshore showed minimum values typical of open ocean data and were consistent with observed nephelometer extinction values and those derived from the measured size distributions to within combined measurement uncertainty. In most cases the lidar data ranged between in-situ tower data for background and breaking wave values and confirms the lidar values are consistent with tower derived ambient extinction values to within the 25% uncertainty identified in this lidar calibration technique.

Acknowledgements:

We extent special appreciation for Drs. R. Ferek and S. Ackleson of the Office of Naval Research for their support [N00014-96-1-0320] of our long-term measurements at BAFS and for the SEAS experiment described here.

REFERENCES

Anderson, T. L. and J.A. Ogren, Determining aerosol radiative properties using the TSI 3563 integrating nephelometer, Aerosol. Sci. Technol., 29, 57-69, 1998

Clarke, A. D. "A Thermo-optic Technique for in-situ Analysis of Size-resolved Aerosol Physicochemistry", Atmos. Env., 25A, 635-644, 1991.

Clarke, A.D., Z. Li and M. Litchy, Aerosol Dynamics in the Pacific Marine Boundary Layer: Microphysics, Diurnal Cycles and Entrainment: *Geophys. Res. Lett.*, 23, pg 733-736, 1996.

Clarke, A., V. Kapustin, The Shoreline Environment Aerosol Study (SEAS-2000): Marine aerosol measurements influenced by a coastal environment and long-range transport, *J.Atmos.Ocean.Technol,* submitted 2002.

Clarke, A., V. Kapustin, S. Howell, K. Moore, B. Lienert, S. Masonis, T. Anderson, D. Covert, K. Shifrin, I. Zolotov, Sea-salt size-distributions from breaking waves: implications for marine aerosol production and optical extinction measurements during SEAS, *J.Atmos.Ocean.Technol,* submitted 2002.

Clarke, A., V. Kapustin and K. Moore, The Contribution of Coastal Aerosol From Breaking Waves to Visible and IR Light-Extinction Over 10 Km Path During RED, Extended Abstract, *12th Conference on Interactions of the Sea and Atmosphere*, AMS, 2003.

de Leeuw, G., F. Neele, M. Hill, M. Smith and E. Vignati, Production of sea-spray aerosol in the surf zone, *J. Geophys. Res*., 29,397-29,409, 2000.

Masonis, S., T. Anderson, D. Covert, V. Kapustin and A. Clarke, A study of extinction to backscatter ratio and its relation to other aerosol optical properties during the SEAS with comparison to polluted site and to Mie Theory, *J.Atmos.Ocean.Technol,* submitted 2002.

Porter, J.N., B. Lienert, and S.K. Sharma, Using the horizontal and slant lidar calibration methods to obtain aerosol scattering coefficients from a coastal lidar in Hawaii, *J. Atmos. Ocean. Tech.,17(11),1445-1454, 2000.*

Porter, J., S. Sharma, B. Lienert and E. Lau, Vertical and Horizontal Aerosol Scattering Fields Over Bellows Beach, Oahu During the SEAS Experiment, *J.Atmos.Ocean.Technol,* submitted 2002.

Tang, I.N., A.C. Tridico, and K.H. Fung , Thermodynamic and optical properties of sea salt aerosol, *J. Geophys. Res., 102*, 23269 – 23275, 1997.

.